

## Sintering behavior of $M_{0.25}Ce_{0.75}O_{1.875}$ (M=Dy, Gd) ceramics fabricated using pulsed electric current sintering method

Hirokazu Suga\*\*\*\*, Toshiyuki Mori\*, Fei Ye\*, Ding Rong Ou\*, Richard Buchanan\*, Toshiyuki Nishimura\*\*, John Drennan\*\*\* and Hidehiko Kobayashi\*\*\*\*

\* Fuel Cell Materials Center, National Institute for Materials Science

Namiki 1-1, Tsukuba, Ibaraki, 305-0044, Japan

E-mail: MORI.Toshiyuki@nims.go.jp

\*\*Nano Ceramics center, National Institute for Materials Science

Namiki 1-1, Tsukuba, Ibaraki, 305-0044, Japan

\*\*\*Centre for Microscopy and Microanalysis, The University of Queensland

St. Lucia, Brisbane, Queensland, 4072, Australia

\*\*\*\*Faculty of Engineering, Saitama University

Shimo-okubo 255, Sakura-ku, Saitama city, Saitama, 338-8570, Japan

Pulsed electric current sintering (PECS) method has been examined for fabrication of dense doped  $CeO_2$  sintered bodies. But high pressure (1GPa) or long time post sintering (>20h) is required in this method. To use this method for development of high quality solid electrolyte in solid oxide fuel cells, the simple PECS process without high pressure or long time post sintering should be developed. In the present study, we examined the influence of particle morphologies and heating rate on PECS behavior.  $M_{0.25}Ce_{0.75}O_{1.875}$  (M=Dy, Gd) powder was prepared by an ammonium carbonate co-precipitation method at 75°C. The relative density of doped  $CeO_2$  PECS specimen increased with an increase of heating rate. The densification behavior of PECS specimen was improved using round shaped particles. It is found that dense PECS specimen (>93% of theoretical density) can be fabricated using nano-size round shaped particles and high heating rate more than 900°C/min.

**Key words:** Doped  $CeO_2$ , Oxide ionic conductor, Pulsed electric current sintering, Heating rate, Particle morphology

### 1 Introduction

Doped  $CeO_2$  is fluorite-related compound which oxide ionic conductivity is higher than yttria stabilized zirconia in oxidizing atmosphere [1, 2]. However, the electronic conductivity in this compound is developed over 600°C in reducing atmosphere. As a consequence of this, the doped  $CeO_2$  has much attention as the electrolyte in solid oxide fuel cells (SOFCs) for intermediate temperature (300-500°C) operation.

Pulsed electric current sintering (PECS) method is a powerful sintering method to achieve a rapid densification under applying pulsed electric current. PECS has been developed for fabrication of the functionally graded materials [3, 4], the composite ceramics [5, 6], the nano-structured ceramics [7] and so on.

In our previous work [8], nano-size round shaped  $Dy_{0.2}Ce_{0.8}O_{1.9}$  powders were prepared using an ammonium carbonate co-precipitation method. The dense  $Dy_{0.2}Ce_{0.8}O_{1.9}$  sintered bodies were fabricated by a combined process of PECS and conventional sintering (CS). However, the relative density of PECS specimen before CS process was less than 87% of theoretical density. A long time (>20h) post CS process was required for fabrication of nano-structured PECS specimen with high density (>98% of theoretical density). The conductivity in this PECS specimen was much higher than that of CS specimen. It is concluded that micro-structure at atomic scale in PECS specimen

became homogeneous by PECS process. To develop this nano-structured solid electrolyte for practical use, however, a proposal of PECS process without post CS process is required.

Anselmi-Tamburini et al. [9] reported the fabrication of dense (>98% of theoretical density)  $Sm_{0.3}Ce_{0.7}O_{1.85}$  sintered at 750°C by PECS without long time post CS process. In this method, high pressure (610MPa) must be applied during PECS. However, high pressure process is also undesirable for industrial applications.

In the present work, we fabricated dense doped  $CeO_2$  sintered bodies using PECS without long post CS process or high pressure process. To improve the relative density of PECS specimens, we examined the influence of powder morphologies and the heating rate on densification process.

### 2 Experimental procedure

#### 2.1 Powder synthesis

The starting materials used were commercially available nitrate powders, cerium nitrate hexahydrate ( $Ce(NO_3)_3 \cdot 6H_2O$ , >99.99% pure, Kanto Chem. Co.), dysprosium nitrate hexahydrate ( $Dy(NO_3)_3 \cdot 6H_2O$ , >99.5% pure, Kanto Chem. Co.), and gadolinium nitrate hexahydrate ( $Gd(NO_3)_3 \cdot 6H_2O$ , >99.95% pure, Kanto Chem. Co.). Nitrate powders were dissolved into distilled water to prepare the composition of  $Ce^{3+}/Dy^{3+}$  (or  $Ce^{3+}/Gd^{3+}$ ) = 3. The concentration of the nitrate solution was 0.15mol/L. Ammonium carbonate

dissolved into distilled water with concentration of 1.5mol/L was used as the precipitant. The nitrate solution was dropped into the precipitant heated at  $75 \pm 1^\circ\text{C}$  while undergoing mild stirring. Then the mixed solution was stirred at the precipitation temperature for 1h. This mixture was filtered by suction filtration and the precipitate was washed five times (three times with distilled water, two times with ethanol). The precipitate was blow-dried for at least 48h with flowing dried nitrogen gas at ambient temperature. The dried solid was crushed in an alumina mortar and pestle, sieved and calcined in flowing oxygen gas for 2h. Calcination temperature ranged from 350-750°C.

## 2.2 Sintering

A PECS unit (Sumitomo Coal Co., DR.SINTER SPS-1030) was used for fabrication of dense sintered bodies. Figure 1 shows a schematic diagram of this sintering unit. Approximately 2g of calcined powder was packed into the graphite mold. The mold was uniaxially pressed at  $500\text{kg}/\text{cm}^2$ . The mold was set on the center of lower electrode in the vacuum chamber and pulsed electric current of 1000A was applied under a load of 60MPa. The heating rate of  $10\text{-}900^\circ\text{C}/\text{min}$  was applied and the sintering temperature was  $1150^\circ\text{C}$  with no holding time.

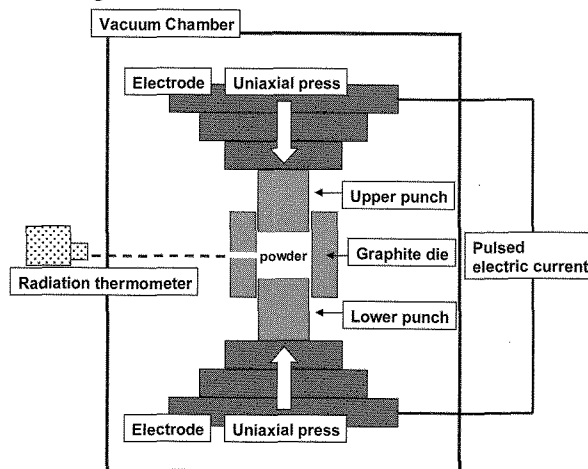


Figure 1 Schematic diagram of pulsed electric current sintering unit.

## 2.3 Characterization

The crystal phases of prepared powders and in sintered bodies were identified using X-ray powder diffraction (XRD). The bulk densities were determined by Archimedes method. The relative density of the sintered body was calculated from the ratio between the bulk density and theoretical density (derived from XRD). The morphologies of powders and the microstructure of sintered bodies were observed by FE-SEM (Hitachi, S-5000). Prior to observation using FE-SEM, sintered bodies were polished and thermally etched for 1 - 2 hours at a temperature  $100^\circ\text{C}$  below sintering temperature. The thermal-etched specimens were coated with platinum. From these images, the mean grain size for each specimen was determined by the average linear intercept method from at least 250 - 300 grains per

specimen [10]. The grain size distribution in the sintered body was plotted using measurement value of grain size.

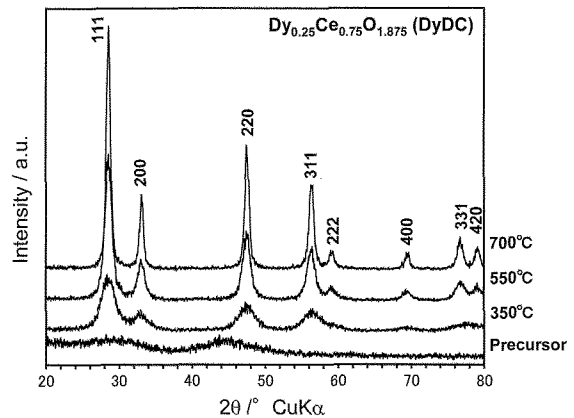


Figure 2 XRD patterns of precursor and calcined powders of  $Dy_{0.25}Ce_{0.75}O_{1.875}$  (DyDC).

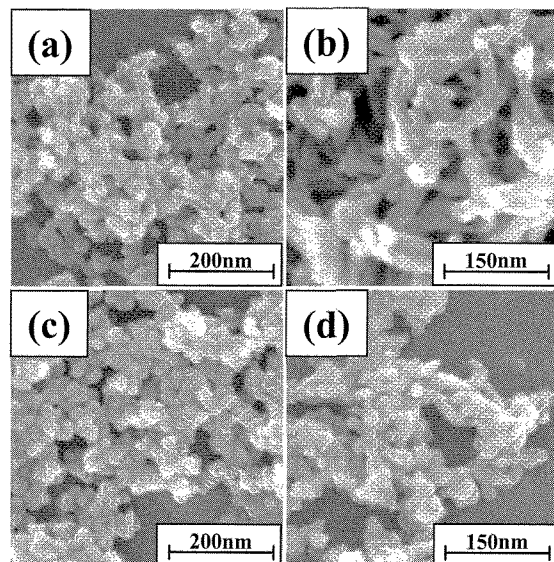


Figure 3 FE-SEM images of precursor powders ((a)DyDC, (b)GdDC) and calcined powders ((c)DyDC, (d)GdDC, calcination temperature:  $700^\circ\text{C}$ ).

## 3 Result and discussion

### 3.1 Powder synthesis

Figure 2 presents XRD patterns of a precursor and calcined powders of 25atom% Dy doped  $CeO_2$  (DyDC). The precursor consists of amorphous like phases. The powder was crystallized over  $350^\circ\text{C}$ . The crystallinity of crystallinity of the calcined powder was improved above  $550^\circ\text{C}$ . The DyDC powders calcined at  $700^\circ\text{C}$  consists of simple fluorite structure. No other phases were observed using XRD. And the influence of calcination temperature of 25atom% Gd doped  $CeO_2$  (GdDC) on its crystallinity was as almost same as the case of DyDC powder. Therefore, the precursor powders of DyDC and GdDC were calcined at  $700^\circ\text{C}$  or  $750^\circ\text{C}$ .

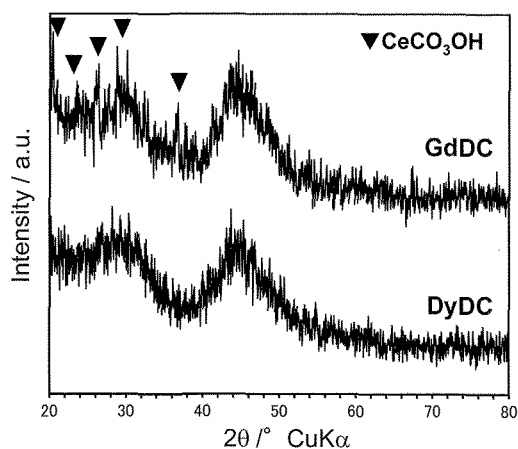


Figure 4 XRD patterns of DyDC and GdDC precursor powders.

FE-SEM images showing the morphology and agglomeration of dried precursors and calcined powders of DyDC and GdDC are shown in Figures 3(a) - 3(d). DyDC precursor and calcined powders were composed of round shaped nano-size particles which average particle size was approximately 30nm. Both precursor and calcined powders showed no morphology difference each other. On the other hand, GdDC precursor consists of the mixture of round shaped and rod-like shaped particles after calcination at 700°C.

To conclude why the morphologies of DyDC and GdDC powders were different, the crystal phases of precursors were carefully assigned as demonstrated in Figure 4. DyDC precursor powder essentially consists of amorphous phases and shows low crystallinity. On the other hand, GdDC precursor included crystallized cerium carbonate hydrate ( $\text{CeCO}_3\text{OH}$ ) phase with orthorhombic symmetry. This indicates that the morphology of rod-like shaped GdDC precursor reflects its crystallographic symmetry. Since DyDC secondary particles were covered by amorphous phases, those

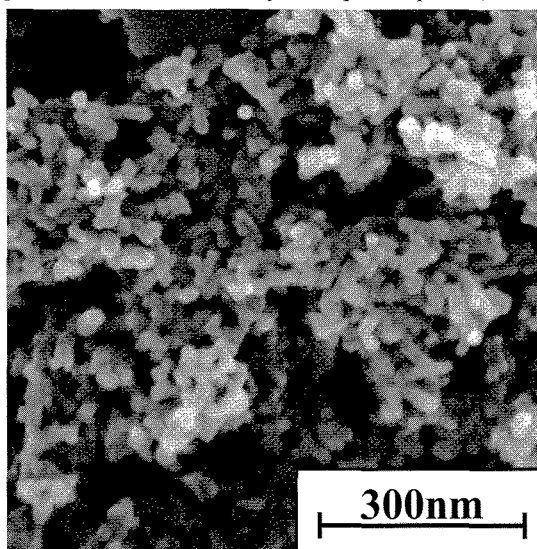


Figure 5 FE-SEM image of GdDC powder calcined at 750°C-2h.

particles look like round shape. In the results of SEM observation, an interesting result is a morphology

change of GdDC powders after calcination. The small round shaped particles came up in SEM image (Fig.3(d)) of calcined GdDC powder. It suggests that small round shaped particles are combined each other and becomes rod-like shaped particles in the precursors. After calcination, some of rod-like shaped aggregates separated into tiny round shaped particles. Furthermore, GdDC powder calcined at higher temperature (750°C-2h) was composed of a lot of round shaped particles as shown in Figure 5. Based on the series of observation results, it is concluded that morphology of doped  $\text{CeO}_2$  particles was influenced by the composition of precursors. The control of morphology and composition of precursors would play an important role in densification process of specimens.

### 3.2 Sintering behavior

Heating rate dependence on relative densities of PECS specimens fabricated using DyDC and GdDC powders calcined at 700°C or 750°C was shown in Figure 6. The relative density of GdDC and DyDC

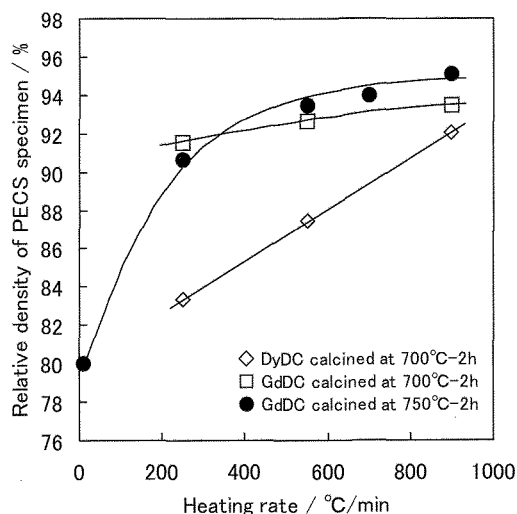


Figure 6 Heating rate dependence on relative densities of PECS specimens fabricated using each calcined powder.

PECS specimens increased with an increase of heating rate in PECS process. GdDC specimen calcined at 750°C was densified up to 95.1% of theoretical density using only rapid PECS process (heating rate: 900°C/min), although GdDC powders calcined at 700°C found difficulty at sintering to high density (>95% of theoretical density) at the same sintering condition due to its relatively low green density.

On the other hand, DyDC specimen calcined at 700°C did not yield dense PECS specimen at 1150°C. It is likely that the green density of aforementioned specimen was too low and would require densification temperature over 1200°C. But doped  $\text{CeO}_2$  is reduced in PECS process above 1200°C. Other alternative powder preparation conditions may be needed to fabricate dense PECS specimens below 1150°C.

These results indicate that low green density of PECS specimen is less favorable for PECS process, while rapid PECS process is useful for densification of DyDC and GdDC specimens. To make dense PECS specimen for fuel cell application, best combination of

particle morphologies and sintering condition be carefully selected.

### 3.3 Microstructure observation

To conclude why high heating rate process is useful for fabrication of dense PECS specimens, microstructures of GdDC PECS and GdDC CS specimens were observed by FE-SEM. Figure 7 compares SEM photographs and histogram of grain size distribution recorded from aforementioned PECS and CS specimens. Figure 7 indicates that CS specimen fabricated at 1150°C with slow heating rate (5°C/min) consists of heterogeneous microstructure. The grain size distribution was broad as compared with PECS specimens. The grain size distribution recorded from

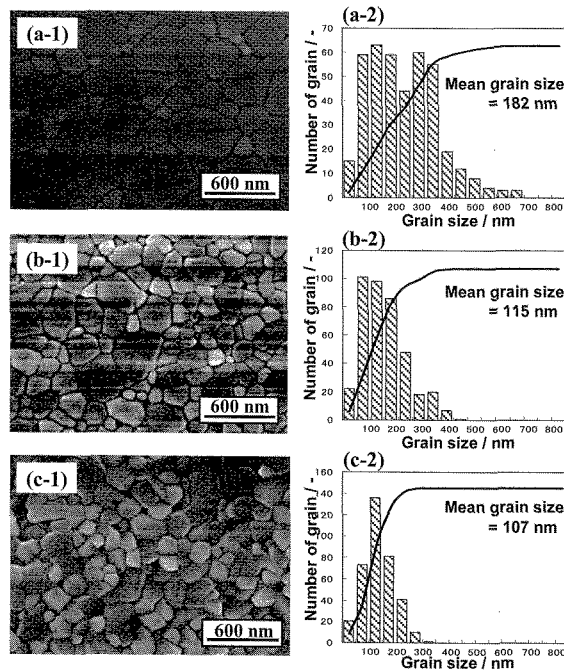


Figure 7 FE-SEM images (a-1, b-1, c-1) and grain size distribution (a-2, b-2, c-2) recorded from GdDC CS specimen (a-1, a-2) and PECS specimens heated at 10°C/min (b-1, b-2) and 900°C/min (c-1, c-2).

PECS specimen fabricated using rapid PECS process (heating rate: 900°C/min) became sharp. Its microstructure looks homogeneous. These results suggest that abnormal grain growth does not allow in PECS specimens. In general, a model of grain growth at intermediate stage of sintering has been discussed using the relationship between grain size distribution of sintered body and its density [11, 12]. According to this model, the grain growth is accelerated by slow heating process. And amount of residual pore in the sintered body is decreased in final stage of sintering. But it is not so easy to minimize the content of residual pore due to heterogeneous grain growth in the specimen. To fabricate the homogeneous microstructure in dense sintered body, cation diffusion around the grain boundaries in sintering process should be simultaneous within specimen. In the conventional sintering process, the specimen is heated from outside of specimen in the furnace. In this case, the simultaneous grain growth in

the specimen is not so easy. On the other hand, the grain boundaries in the specimen are directly heated by applied current in PECS process. The cation diffusion around grain boundary would be simultaneous in whole specimen. This would lead microstructure of PECS specimens to homogenous. In addition, the high heating rate in PECS process can be controlled by enhancement of applied current level. This indicates that high heating rate process provides the grain boundary much amount of energy for cation diffusion in PECS process. As a consequence of this, the homogeneity of microstructure in GdDC PECS specimen fabricated using high heating rate 900°C/min was the best in all observed specimens. Based on these results and conclusion, it is concluded that a control of PECS parameters (i.e. on-set time of pulse current, amount of applied pulse current and so on) would play an important role for fabrication of homogeneous micro-structure in the sintered bodies.

### 4. Summary

To fabricate dense doped  $CeO_2$  specimens by PECS, the influence of morphologies of calcined powders and heating rate in PECS process on the density and microstructure of specimen was examined. The relative density of PECS specimen increased with an increase of heating rate in PECS process. GdDC specimen calcined at 750°C was densified up to 95.1% of theoretical density using only rapid PECS process (heating rate: 900°C/min) without long post CS or high pressure. Also the specimen with high green density can be easily densified in PECS process. These results suggest that both of morphology control of powders and optimization of PECS parameters contribute to fabrication of homogeneous microstructure of doped  $CeO_2$ . It is expected that the present PECS process will provide us chance to create nano-structured doped  $CeO_2$  solid electrolyte with high oxide conductivity in SOFCs.

### References

1. S.M.Haile, *Acta Materialia*, **51**, 5981-6000(2003).
2. V.V.Kharton, F.M.B.Marques and A. Atkinson, *Solid State Ionics*, **174**, 135-149(2004).
3. H.Guo, K.A.Khor, Y.C.Boey and X.Miao, *Biomaterials*, **24**, 667-675(2003).
4. Y.J.Wu, N.Uekawa and K.Kakegawa, *Mat.Letters*, **57**, 4088-4092(2003).
5. L.Gao, H.Z.Wang, J.S.Hong, H.Miyamoto, K.Miyamoto, Y.Nishikawa and S.D.D.L.Torre, *J.Eur.Ceram.Soc.*, **19**, 609-613(1999).
6. J.F.Li, S.Satomi, R.Watanabe, M.Omori and T.Hirai, *J.Eur.Ceram.Soc.*, **20**, 1795-1802(2000).
7. R.Chaim, R.Marder-Jaechel and J.Z.Shen, *Mat.Sci.Eng. A*, **429**, 74-78(2006).
8. T.Mori, T.Kobayashi, Y.Wang, J.Drennan, T.Nishimura, J.G.Li and H.Kobayashi, *J.Am.Ceram.Soc.*, **88**[7], 1981-1984(2005).
9. U.Anselmi-Tamburini, J.E.Garay and Z. A. Munir, *Scripta Materialia*, **54**, 823-828 (2006).
10. M. I. Mendelson, *J.Am.Ceram.Soc.*, **52**[8], 443-446 (1969).
11. T.Ikegami, M.Tsutsumi, S.Matsuda and S.Shirasaki, *J.App.Phys.*, **49**[7], 4238-4211 (1978).
12. T.Ikegami, and Y.Moriyoshi, *J.Am.Ceram.Soc.*, **68**[11], 597-603 (1985).